CrossMark
click for updates

# Microwave assisted synthesis of MoS₂/nitrogen-doped carbon shell–core microspheres for Pt-free dye-sensitized solar cells

Guang Zhu,*[a] Haifeng Xu,[a] Hongyan Wang,[a] Wenqi Wang,[a] Quanxin Zhang,[c] Li Zhang[a] and Hengchao Sun*[b]

In this work, novel MoS₂/nitrogen-doped carbon shell–core microspheres (MNCS) have been designed and prepared through the microwave-assisted method, and used as counter electrodes for platinum-free dye-sensitized solar cells (DSSCs). The results show that as-prepared shell–core composite microspheres possess low charge transfer resistance and high electrocatalytic activity. When used as a counter electrode for DSSCs, the powder conversion efficiency of an as-prepared cell with optimized MNCS reaches 6.2% under standard light illumination, which is comparable to cells with a conventional Pt counter electrode.

## Introduction

In the development of clean energy, solar energy is a plentiful and environmentally safe energy source. In recent years, dye-sensitized solar cells (DSSCs) have attracted considerable attention as an alternative to conventional silicon based solar cells due to their low cost, easy fabrication and high power conversion efficiency.[1–8] A typical DSSC is composed of a photoanode, an electrolyte, and a counter electrode. Among them, the counter electrode (CE) reduces the oxidized electrolyte, which is critical for high performance DSSCs.[9–12] So far, platinum is still the most widely-used CE for DSSCs due to its excellent electrical conductivity and high catalytic activity.[13–20] However, the use of noble Pt metal would be limited by the scarcity and high cost. Therefore, it is necessary to explore the low cost and Pt-free CEs to facilitate the industrial development of DSSCs.

As a typical layered transition metal sulfide, molybdenum disulfide (MoS₂) has attracted considerable attention and was proposed as an effective candidate counter electrode to replace Pt for DSSCs due to its analogous structure to graphene.[21,22] However, the drawback of MoS₂ is that its active sites are limited to its edges, which decreases the DSSC's performance.[23–26] Recently, some works have demonstrated that MoS₂ incorporated with carbon composites could lower the charge transfer resistance and enhance the electrocatalytic activity, which can

improve the photovoltaic performance.[27–31] Tai *et al.* prepared multi-walled carbon nanotubes (MWCNTs) and MoS₂ nanocomposites as counter electrodes for DSSCs, and a conversion efficiency of 6.41% was obtained.[32] Liu *et al.* prepared MoS₂ and graphene composite by simply mixing graphene oxide nanosheets with MoS₂ as counter electrodes and a conversion efficiency of 6.04% was achieved.[33] Yue *et al.* fabricated MoS₂/carbonaceous hybrid material by a hydrothermal route as CE materials for DSSCs, and showed a photovoltaic efficiency of 7.69%.[34] Despite the above process has been achieved, the design and fabrication of MoS₂ incorporated with carbon material composites with high electrocatalytic activity for DSSCs are still very challenging.

In our previous work, the nitrogen-doped carbon microspheres (NCS) were prepared *via* a simple, rapid and effective microwave assisted method and used as CEs for DSSCs. To further expand the application of this method in DSSCs, herein we report the fabrication of novel MoS₂/nitrogen-doped carbon shell–core microspheres (MNCS) *via* all microwave assisted method for DSSCs. To our knowledge, there are rare research reports on enhanced photovoltaic performance of DSSCs based on the type of MoS₂/nitrogen-doped carbon shell–core microspheres CEs. It is found that as-prepared MNCS can lower the charge transfer resistance and enhance the electrocatalytic activity. When it serves as the CEs in DSSCs, a high conversion efficiency of 6.2% can be achieved under one sun illumination, which is comparable to the cell with conventional Pt counter electrode.

## Experimental

NCS was fabricated *via* the microwave-assisted method reported in our previous work.[35] Subsequently, the MNCS was fabricated

[a] *Anhui Key Laboratory of Spin Electron and Nanomaterials, Suzhou University, Suzhou 234000, P. R. China. E-mail: guangzhu@ahsztc.edu.cn; Fax: +86-557-2871003; Tel: +86-557-2871006*

[b] *Institute of Microelectronics, Chinese Academy of Science, Beijing 100029, P. R. China. E-mail: sunhengchao@ime.ac.cn*

[c] *Lanzhou Institute of Chemical Physics, Chinese Academy of Sciences, Lanzhou 730000, P. R. China*

*via* microwave-assisted method again. In brief, the appropriate amount of as-prepared NCS was dissolved in 100 ml of 20 mM trioxomolybdenum-phosphoric solution, and then followed by ultrasonication for 30 min. And then, 100 ml of 70 mM thio-acetamide was added into the reaction solution under stirring. After that, the above solution was heated at 160 °C with a microwave irradiation power of 100 W for 10 min using a microwave system (Explorer-48, CEM Co.). After being centrifuged and washed with deionized water, the resultant precipitate was dried in a vacuum oven at 120 °C for 12 h, and finally thermally treated at 800 °C for 2 h in an ammonia atmosphere. In this work, the amount of NCS was set as 53.3 mg, 80 mg, and 160 mg, and the corresponding obtained samples are denoted as MNCS-1, MNCS-2, and MNCS-3, respectively. The MNCS counter electrode was prepared by drop coating method on the cleaned F-doped $SnO_2$ (FTO) glass. In addition, the pure $MoS_2$ and conventional Pt counter electrodes were prepared for comparison. The DSSCs devices with the active area of 0.2 $cm^2$ were assembled and fabricated based on our previous work.[35]

The surface morphologies of the samples were measured by the JEOL JSM-LV5610 field emission scanning electron microscopy (FESEM) and JEOL-2010 high-resolution transmission electron microscopy (HRTEM), respectively. Nitrogen adsorption–desorption isotherms were measured at 77 K with an ASAP 2020 Accelerated Surface Area and Porosimetry System (Micrometitics, Norcross, GA). The compositions of the samples were analyzed by a Holland Panalytical PRO PW3040/60 X-ray diffraction (XRD) with Cu Kα radiation ($V$ = 30 kV, $I$ = 25 mA). Cyclic voltammetry (CV) measurements were carried out by an electrochemical workstation (Autolab PGSTAT 302N) in a three electrode electrochemical system, which contained an ACN solution of 10 mM LiI, 1.0 mM $I_2$, and 0.1 M $LiClO_4$. Electrochemical impedance spectroscopy (EIS) measurements were performed by the above mentioned electrochemical workstation under 100 mW $cm^{-2}$ illumination at an applied bias of $V_{oc}$, applying a 10 mV AC sinusoidal signal over the constant applied bias with the frequency ranging between 100 kHz and 0.1 Hz. The performance of as-prepared devices was measured by a Newport solar simulator fitted with an AM 1.5 G filter, in conjunction with a Keithley 2440 source meter.

## Results and discussion

The morphologies of the as-prepared NCS and MNCS were investigated by FESEM. Fig. 1a shows the morphology of the as-prepared NCS. It can be observed that these nitrogen-doped carbon microspheres are quite uniform and monodispersed, with an average diameter of around 2 μm. Compared with pure nitrogen-doped carbon microspheres, a out-layer of $MoS_2$ with a thickness of *ca.* 200 nm can be observed on the surface of microspheres. The results indicate that the shell–core structured $MoS_2$/nitrogen-doped carbon microspheres were fabricated *via* microwave assisted method. Fig. 2 shows the HRTEM image of as-prepared MNCS. The lattice from $MoS_2$ outlayer can observed clearly. The interlayer spacing of 0.62 nm observed
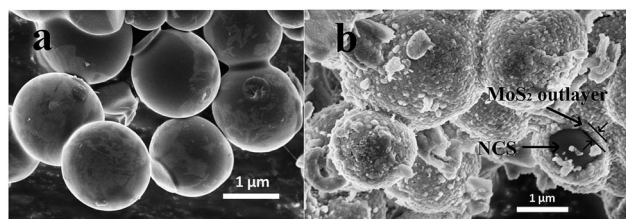


**Fig. 1** FESEM images of the as-prepared (a) nitrogen-doped carbon microspheres and (b) $MoS_2$/nitrogen-doped carbon shell–core microspheres.

from lattice fringes can be ascribed to the (002) direction of hexagonal $MoS_2$

Fig. 3 shows the $N_2$ adsorption–desorption isotherms of as-prepared $MoS_2$ and MNCS-2. The Brunauer–Emmet–Teller (BET) specific surface area and mean pore diameter were determined and summarized in Table 1. As seen, the MNCS-2 shows a higher BET specific surface area (35.39 $m^2$ $g^{-1}$) and larger pore volume (16.02 nm) than $MoS_2$ (2.64 $m^2$ $g^{-1}$ and 9.52 nm), respectively. The greatly enhanced specific surface area provides more active plots to reduce $I_3^-$.

The phase structure of the as-synthesized pure $MOS_2$ and MNCS composites with different NCS amounts was further characterized by using XRD. As shown in Fig. 4, all samples exhibit a hexagonal $MoS_2$ crystal structure (JCPDS 75-1539). Moreover, the strong (002) diffraction peak at 14.4° can be observed in samples, indicating a well stacked layered structure of $MOS_2$.[36] The broad peaks at 24° corresponds to (002) diffraction mode of graphitic structure, which is characteristic of disordered carbon material.[37,38] It is noted that the (002) diffraction peak gradually becomes weak with the decrease of NCS amount. The results further confirm that $MoS_2$/nitrogen-doped carbon composite microspheres can be fabricated *via* this method.

CV measurements were carried out to analyze the electrochemical catalytic activity of as-prepared electrodes. Fig. 5 indicates the CV curves of the pure $MoS_2$, various MNCSs and Pt counter electrodes under the potential from −0.5 to 1.2 V for the $I_3^-/I^-$ redox couple. Two pairs of oxidation and
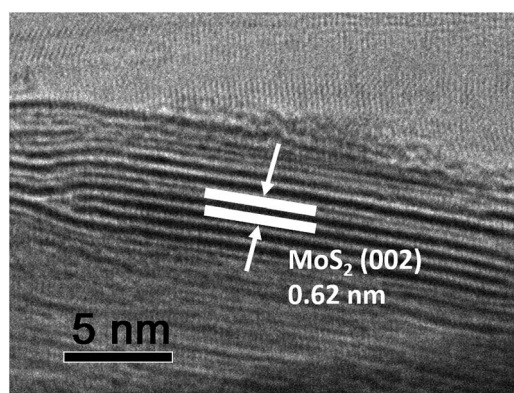


**Fig. 2** The HRTEM image of as-prepared $MoS_2$/nitrogen-doped carbon shell–core microspheres.
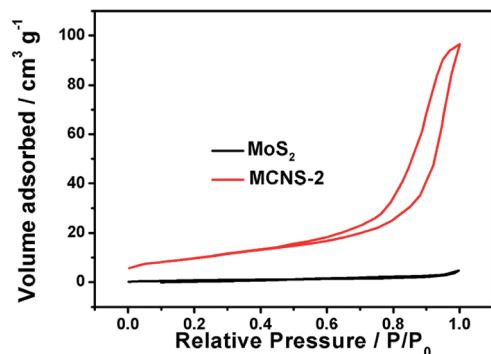
Fig. 3 Nitrogen adsorption–desorption isotherms of as-prepared $MoS_2$ and MNCS-2.

Table 1 Specific surface area and mean pore diameter of as-prepared $MoS_2$ and MCNS-2

| Sample | Specific surface area/m² g⁻¹ | Mean pore diameter/nm |
|---|---|---|
| $MoS_2$ | 2.64 | 9.52 |
| MNCS-2 | 35.39 | 16.02 |

reduction peaks are observed, which are assigned to the following reactions.[39,40]

$$3I^- \leftrightarrow I_3^- + 2e^- \quad (1)$$

$$2I_3^- \leftrightarrow 3I_2 + 2e^- \quad (2)$$

The peak positions of the CV curves for as-prepared MNCS electrodes are similar to that of Pt, indicating that MNCS electrodes have a similar electrocatalytic function for the redox reaction to Pt electrode. Among these electrodes, MNCS-2 indicates higher current density than other electrodes based on $MoS_2$, which could be due to the larger specific surface area and higher reactivity in MCNS-2 electrode for catalysis.[41]
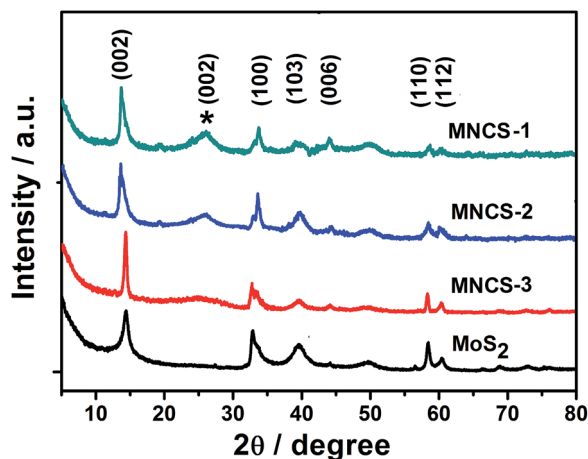


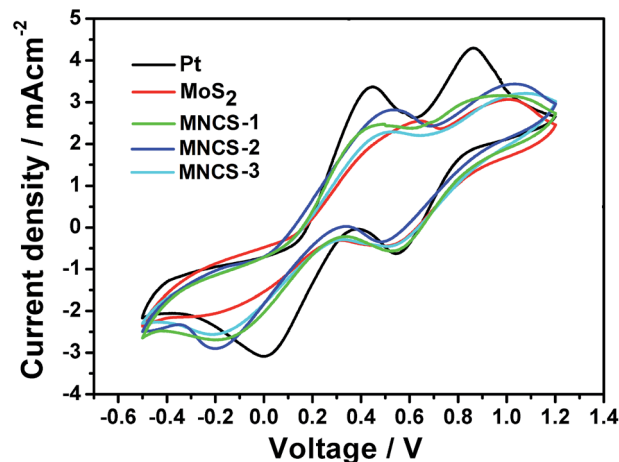Fig. 4 XRD patterns of as-prepared pure $MOS_2$ and MNCS composites.



Fig. 5 CV curves of the pure $MoS_2$, various MNCSs and Pt counter electrodes.

Fig. 6 displays the typical EIS spectra of the cells with various counter electrodes. Two semicircles, including a large one at high frequency and a small one at low frequency, can be observed in the Nyquist plots of EIS spectra. The left semicircle at high frequency represents the charge-transfer resistance ($R_{CT}$) and the corresponding capacitance ($CPE_1$) at the interface of the electrolyte/counter electrode. The right semicircle at low frequency represents the charge-transfer resistance ($R_w$) and corresponding capacitance ($CPE_2$) at the $TiO_2$/dye/electrolyte interface.[42] As listed in Table 2, the fitted $R_{CT}$ values of pure $MoS_2$, MNCS-1 and MNCS-3 CEs are 20.1, 8.8 and 7.8 Ω, respectively. However, as for the MNCS-2 CE (6.1 Ω) is lower than that of Pt CE (7.2 Ω), indicating its high electrocatalytic performance. The low $R_{CT}$ value indicates superior electrocatalytic activity for $I_3^-$ reduction, which is beneficial to the fill factor and conversion efficiency.

The $J$–$V$ curves of DSSCs with various CEs were measured under one sun illumination (100 mW cm⁻², AM 1.5 G) and showed in Fig. 7. The corresponding photovoltaic parameters, such as the open circuit potential ($V_{oc}$), short circuit current density ($J_{sc}$), fill factor (FF), and conversion efficiency ($\eta$) are
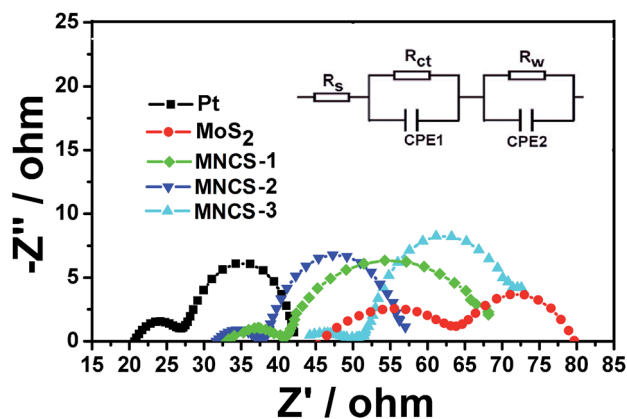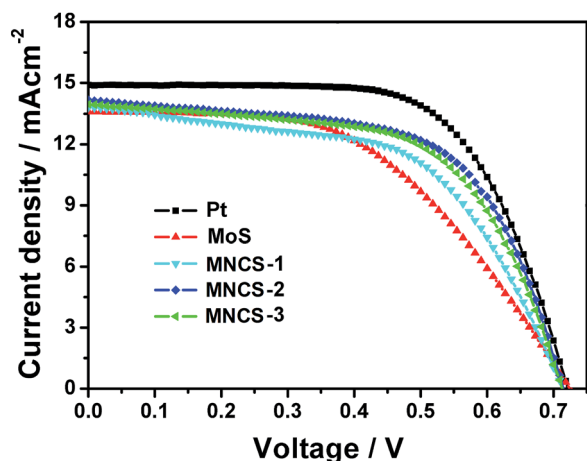


Fig. 6 EIS spectra of the pure $MoS_2$, various MNCSs and Pt counter electrodes, the inset is the corresponding equivalent circuit.

**Table 2** Photovoltaic parameters of the cells with various counter electrodes

| Sample | $R_{CT}/\Omega$ | $J_{sc}/\text{mA cm}^{-2}$ | $V_{oc}/\text{V}$ | FF/% | $\eta$/% |
|---|---|---|---|---|---|
| Pt | 7.2 | 14.9 | 0.72 | 65.2 | 7.0 |
| MoS$_2$ | 20.1 | 13.6 | 0.72 | 50.8 | 5.0 |
| MNCS-1 | 8.8 | 14.0 | 0.71 | 60.2 | 6.0 |
| MNCS-2 | 6.1 | 14.2 | 0.71 | 61.3 | 6.2 |
| MNCS-3 | 7.8 | 13.8 | 0.71 | 56.2 | 5.5 |



**Fig. 7** $J$–$V$ curves of DSSCs with various CEs.

listed in Table 2. The $J_{sc}$ and FF of the cell with pure MoS$_2$ are 13.6 mA cm$^{-2}$ and 50.8%, respectively, resulting in a low conversion efficiency of 5.0%. When nitrogen-doped carbon microspheres are introduced, $J_{sc}$, FF and $\eta$ increase obviously and reach maximum values of 14.20 mA cm$^{-2}$, 61.3% and 6.2% for the cell with MNCS-2 CE, which is due to the high electro-catalytic activity and low charge transfer resistance resulting from the interaction between nitrogen-doped carbon microspheres and MoS$_2$. However, conversion efficiency will decreases with a further increase of nitrogen-doped carbon microspheres amount, which is ascribed to reduced electro-catalytic activity resulting from the excessive nitrogen-doped carbon microspheres. Despite the maximum $\eta$ of 6.2% for the cell with MNCS-2 CE is lower than that of Pt CE (7.0%). However, considering the low cost and superior chemical stability of MNCS composites, the MNCS CEs are still competitive to conventional Pt CE.

## Conclusion

In summary, MoS$_2$/nitrogen-doped carbon shell–core microspheres have been synthesized through a microwave-assisted method and used as a Pt-free counter electrode in DSSCs. The results indicate that as-prepared composite counter electrodes exhibit high electrocatalytic activity and low charge transfer resistance resulting from the interaction between nitrogen-doped carbon microspheres and MoS$_2$. Under optimal conditions, a maximum photovoltaic conversion efficiency of 6.2%

under one sun illumination is achieved for DSSCs with MNCS-2 CE, which is comparable to that for conventional Pt counter electrode. That suggests that as-prepared MNCS composite CEs show great potential as a low cost alternative to Pt for DSSCs.

## Acknowledgements

## Notes and references

1 M. Gratzel, *Nature*, 2001, **414**, 338.
2 C. Zha, L. Shen, X. Zhang, Y. Wang, B. A. Korgel, A. Gupta and N. Bao, *ACS Appl. Mater. Interfaces*, 2013, **6**, 122.
3 X. Huang, D. Qin, X. Zhang, Y. Luo, S. Huang, D. Li and Q. Meng, *RSC Adv.*, 2013, **3**, 6922.
4 G. Zhu, L. K. Pan, T. Lu, T. Xu and Z. Sun, *J. Mater. Chem.*, 2011, **21**, 14869.
5 H. Chen, D. Kou, Z. Chang, W. Zhou, Z. Zhou and S. Wu, *ACS Appl. Mater. Interfaces*, 2014, **6**, 20664.
6 D. S. Yang, C. Kim, M. Y. Song, H. Y. Park, J. C. Kim, J. J. Lee, M. J. Ju and J. S. Yu, *J. Phys. Chem. C*, 2014, **118**, 16694.
7 H. Sun, D. Qin, S. Huang, X. Guo, D. Li, Y. Luo and Q. Meng, *Energy Environ. Sci.*, 2011, **4**, 2630.
8 X. J. Sang, J. S. Li, L. C. Zhang, Z. M. Zhu, W. L. Chen, Y. G. Li, Z. M. Su and E. B. Wang, *Chem. Commun.*, 2014, **50**, 14678.
9 R. Jia, J. Chen, J. Zhao, J. Zheng, C. Song, L. Li and Z. Zhu, *J. Mater. Chem.*, 2010, **20**, 10829.
10 S. Hou, X. Cai, H. Wu, X. Yu, M. Peng, K. Yan and D. Zou, *Energy Environ. Sci.*, 2013, **6**, 3356.
11 Y. Xue, J. Liu, H. Chen, R. Wang, D. Li, J. Qu and L. Dai, *Angew. Chem., Int. Ed.*, 2012, **51**, 12124.
12 L. Song, Q. Luo, F. Zhao, Y. Li, H. Lin, L. Qu and Z. Zhang, *Phys. Chem. Chem. Phys.*, 2014, **16**, 21820.
13 M. Tathavadekar, M. Biswal, S. Agarkar, L. Giribabu and S. Ogale, *Electrochim. Acta*, 2014, **123**, 248.
14 M. Wu, X. Lin, T. Wang, J. Qiu and T. Ma, *Energy Environ. Sci.*, 2011, **4**, 2308.
15 S. Pan, Z. Yang, P. Chen, X. Fang, G. Guan, Z. Zhang, J. Deng and H. Peng, *J. Phys. Chem. C*, 2014, **118**, 16419.
16 M. Y. Yen, C. K. Hsieh, C. C. Teng, M. C. Hsiao, P. I. Liu, C. C. M. Ma, M. C. Tsai, C. H. Tsai, Y. R. Lin and T. Y. Chou, *RSC Adv.*, 2012, **2**, 2725.
17 H. C. Sun, T. Q. Chen, Y. Liu, X. Hou, L. Zhang, G. Zhu, Z. Sun and L. K. Pan, *J. Colloid Interface Sci.*, 2015, **445**, 326.
18 Y. Bai, X. Zong, H. Yu, Z. G. Chen and L. Wang, *Chem.–Eur. J.*, 2014, **20**, 8670.
19 M. Wu, X. Lin, Y. Wang, L. Wang, W. Guo, D. Qi, X. Peng, A. Hagfeldt, M. Gratzel and T. Ma, *J. Am. Chem. Soc.*, 2012, **134**, 3419.

20 F. Gong, H. Wang, X. Xu, G. Zhou and Z. S. Wang, *J. Am. Chem. Soc.*, 2012, **134**, 10953.

21 S. Hussain, S. F. Shaikh, D. Vikraman, R. S. Mane, O.-S. Joo, M. Naushad and J. Jung, *ChemPhysChem*, 2015, **16**, 3959.

22 A. Antonelou, G. Syrrokostas, L. Sygellou, G. Leftheriotis, V. Dracopoulos and S. N. Yannopoulos, *Nanotechnology*, 2016, **27**, 045404.

23 L. Sanchez, D. Lembke, M. Kayci, A. Radenovic and A. Kis, *Nat. Nanotechnol.*, 2013, **8**, 497.

24 Q. Xiang, J. Yu and M. Jaroniec, *J. Am. Chem. Soc.*, 2012, **134**, 6575.

25 R. Ganatra and Q. Zhang, *ACS Nano*, 2014, **8**, 4074.

26 M. L. Tsai, S. H. Su, J. K. Chang, D. S. Tsai, C. H. Chen, C. I. Wu, L. J. Li, L. J. Chen and J. H. He, *ACS Nano*, 2014, **8**, 8317.

27 Z. Chen, A. J. Forman and T. F. Jaramillo, *J. Phys. Chem. C*, 2013, **117**, 9713.

28 G. T. Yue, J. Y. Lin, S. Y. Tai, Y. Xiao and J. H. Wu, *Electrochim. Acta*, 2012, **85**, 162.

29 Y. J. Tang, Y. Wang, X. L. Wang, S. L. Li, W. Huang, L. Z. Dong, C. H. Liu, Y. F. Li and Y. Q. Lan, *Adv. Energy Mater.*, 2016, **6**, 1600116.

30 S. A. Patil, P. Y. Kalode, R. S. Mane, D. V. Shinde, A. Doyoung, C. Keumnam, M. M. Sung, S. B. Ambade and S. H. Han, *Dalton Trans.*, 2014, **43**, 5256.

31 W. Wei, K. Sun and Y. H. Hu, *J. Mater. Chem. A*, 2016, **4**, 12398.

32 S. Y. Tai, C. J. Liu, S. W. Chou, F. S. Chien, J. Y. Lin and T. W. Lin, *J. Mater. Chem.*, 2012, **22**, 24753.

33 C. J. Liu, S. Y. Tai, S. W. Chou, Y. C. Yu, K. D. Chang, S. Wang, F. S. Chien, J. Y. Lin and T. W. Lin, *J. Mater. Chem.*, 2012, **22**, 21057.

34 G. T. Yue, J. H. Wu, Y. M. Xiao, M. L. Huang, J. M. Lin and J. Y. Lin, *J. Mater. Chem. A*, 2013, **1**, 1495.

35 G. Zhu, H. Y. Wang, H. Xu, Q. Zhang, H. Sun and L. Zhang, *RSC Adv.*, 2016, **6**, 58064.

36 Z. Wu, B. Fang, Z. Wang, C. Wan, Z. Liu, F. Liu, W. Wang, A. Alfantazi, D. Wang and D. P. Wilkinson, *ACS Catal.*, 2013, **3**, 2101.

37 T. Q. Chen, L. K. Pan, T. Loh, Y. F. Yao, Q. Chen, D. S. Li, W. Qin and Z. Sun, *Dalton Trans.*, 2014, **43**, 14931.

38 T. Q. Chen, L. K. Pan, X. J. Liu and Z. Sun, *Mater. Chem. Phys.*, 2013, **142**, 345.

39 G. Boschloo and A. Hagfeldt, *Acc. Chem. Res.*, 2009, **42**, 1819.

40 J. D. Roy Mayhew, D. J. Bozym, C. Punckt and I. A. Aksay, *ACS Nano*, 2010, **4**, 6203.

41 P. Li, J. Wu, J. Lin, M. Huang, Y. Huang and Q. Li, *Sol. Energy*, 2009, **83**, 845.

42 G. Zhu, L. K. Pan, H. C. Sun, X. J. Liu, T. Lv, T. Lu, J. Yang and Z. Sun, *ChemPhysChem*, 2012, **13**, 769.